2016

MODELING, SIMULATION AND CONTROL OF HYBRID ELECTRIC VEHICLE DRIVE WHILE MINIMIZING ENERGY INPUT REQUIREMENTS USING OPTIMIZED GEAR RATIOS

Sanjai Massey
Michigan Technological University, smassey@mtu.edu

MODELING, SIMULATION AND CONTROL OF HYBRID ELECTRIC VEHICLE DRIVE WHILE MINIMIZING ENERGY INPUT REQUIREMENTS USING OPTIMIZED GEAR RATIOS

By

Sanjai Massey

A REPORT

Submitted in partial fulfillment of the requirements for the degree of

MASTER OF SCIENCE

In Electrical Engineering

MICHIGAN TECHNOLOGICAL UNIVERSITY

2016

This report has been approved in partial fulfillment of the requirements for the Degree of MASTER OF SCIENCE in Electrical Engineering.

Department of Electrical and Computer Engineering

Report Advisor: *Wayne Weaver*

Committee Member: *Lucia Gauchia*

Committee Member: *John Lukowski*

Department Chair: *Daniel R. Fuhrmann*

Contents

List of Figures

List of Tables

Acknowledgements

I am very grateful to my advisor, Dr. Wayne Weaver, for the guidance and support. Without his guidance and motivation, this work could not have been completed.

I am also thankful to my family and friends who helped and supported me in completing the research work.

I also thank the committee members who accepted my proposal and allowed me to research on the topic which I have presented in the meeting.

List of Abbreviations

AC	Alternating Current
CPU	Central Processing Unit
CVT	Continuous Variable Transmission
DC	Direct Current
DOE	Department of Energy
ECU	Electronic Control Unit
EPA	Environmental Protection Agency
EV	Electric Vehicle
EM	Electric Motor
HEV	Hybrid Electric Vehicle
ICE	Internal Combustion Engine
IDC	Indian Drive Cycle
IGBT	Insulated Gate Bipolar Transistor
IM	Induction Motor
MOSFET	Metal Oxide Semi-conductor Field Effect Transistor
NHTSA	National Highway Transportation Safety Administration
SOC	State of Charge
P_{ICE}	Power from Internal Combustion Engine
PID	Proportional Integral Differentiator
PMSM	Permanent Magnet Synchronous Motor
PSD	Power Split Device
P_{TM}	Power from Torque Motor
RPM	Revolutions per Minute
UDDS	Urban Dynamometer Driving Schedule
VSD	Variable Speed Drive

Abstract

This project was conducted to analyze (model and simulate) and optimize an electric motor based drive system to propel a typical passenger vehicle in an urban driving environment. Although there are many HEV and EV type systems on the market today, this paper chose the Toyota Prius HEV system as a baseline using a brushless AC motor.

Although a vehicle can be driven many ways, a more standardized Urban Dynamometer Driving Schedule, UDDS, was chosen to simulate real driving conditions. This schedule is determined by the US Environmental Protection Agency, EPA, and is intended to represent the city driving conditions for a typical passenger vehicle in a city environment.

A high level modeling and simulation approach for vehicle and motor drive was taken to focus on motor operation and gear ratios from the electric to the mechanical drive system.

Vehicle battery being the limiting factor in the range of the HEV vehicle, the energy usage of the battery was optimized to ensure lowest energy dissipation, thus gaining the most mileage out of the vehicle.

How to maximize the drive mileage for a given battery size? There are multiple dynamic factors that affect the battery usage and efficiency. Factors such as road conditions, vehicle speed, weather, weight, and aerodynamics are amongst the many that govern battery mileage. Gear ratios and selection also play a crucial role in the loading and efficiency of the motor, thus affecting the battery mileage.

In this project, the gear ratios between the electric motor and the vehicle drive shaft were the focus for this optimization. As part of the overall system model, gears and gear ratios were modeled and simulated to determine their optimum ratios for finding the minimum energy usage point for the battery.

1 Introduction

The concept of battery operated Hybrid Electric Vehicles (HEV) and full Electric Vehicles (EV) are as old as the automobile itself from over hundred years ago. Unfortunately, the low cost of fossil fuels subdued any traction these vehicles may have had. The last decade, though, has been a boom to the EV market, as they have become a growing market segment in the transportation space. The main reasons have been to reduce the impact of burning fossil fuels on the environment, lower transportation operating costs, and general consumer interest in technology [1].

There is now sufficient momentum from the auto makers, that even the reduced fuel costs for the internal combustion engine (ICE) cars, will not be able to stop the progress and proliferation on HEVs and EVs. In fact, electrification of vehicles has now become the basis from which to launch new technologies in automobiles such as semi-autonomous and even autonomous driving.

Although computer models have been used for decades in the design industry, the onset of next generation EVs has really accelerated the use of computer modeling and simulation of the whole system to optimize all aspects of vehicles, including energy consumption. This has become extremely important since the battery charging stations cannot be found as readily as gas stations. A battery also takes much longer to charge than filling a gas tank in an internal combustion engine, ICE, vehicle.

The work in this paper has been inspired by the work done by Oak Ridge National Laboratory at the U.S. Department of Energy (DOE) in which a 2010 Toyota Prius hybrid automobile was studied and analyzed. The results of this study are published in the paper titled “Evaluation of 2010 Toyota Prius Hybrid Synergy Drive System” prepared by Mitch Olszewski, program manager [2].

This was a thorough evaluation of the vehicle by means of a complete tear down of the motor drive system, where all aspects of the sub-systems were tested for performance Goals of this evaluation were to characterize the performance of the electical and mechanical system, including the inverter/motor sub-system [2].

Although, a review of the DOE evaluation of the Prius hybrid is beyond the scope of this paper, it, however, does serve as a foundatation for this project to further the learning, and thus optimizing the design for energy consumption.

In the last three decades, there has been research on the fuel consumption of vehicles through technical changes. The impact of behavioral characteristics has not been researched that much in the areas of fuel consumption of the vehicles. Real driving cycles are different from the predefined cycles which is shown from the empirical studies.

A more recent study showed how a realistic drive cycle can be used to optimize gear ratios where dynamics of the driving is taken into account [3]. Research was done using Indian city roads with Indian Driving Cycle (IDC). This study showed that optimal coordination of both gear ratio and speed of vehicle has an important role in improving the fuel efficiency of vehicle.

Understanding the limits of the actual components now allow us to correctly model the critical sub-systems at high level and to simulate the real world driving environment. The computer models and simulations can be run for multiple variations of the key parameters that may effect the system performance, and then allowed to determine the optimum operating points without building multiple prototypes, and running actual field tests, which can be time consuming and costly.

Two important factors must be considered before attemping to simulate computer models of the desired subsystems. First is to obtain the mathematical equations that define the physical behavior of electric drive sub-systems. Second is to determine the level of complexity that the models need to be to provide relevant information. Since all models are an approximations of behaviors, it is important to understand what is expected from the simulations and modeling only what is required to provide relevant results.

2 Background

HEV is defined as the technology in which there are more than one energy source used in which at least one source will be electricity. There are three main type of HEVs. All HEV systems are equipped with an electric motor, an ICE and a generator. They may be considered either series, parallel, or series-parallel depending on how the system is configured. Series hybrid is very similar to an EV, in that the electric motor moves the vehicle. The gasoline engine is there only to provide added power to the motor via the inverter, and acts as a range extender.

A parallel hybrid is where the power to the drivetrain is shared by ICE and the motor. The concept of using the parallel hybrid system is successfully implemented in the new Honda Insight improved model and in Honda Civic Hybrid. The advantages of using Parallel hybrid source is that if any of the source of power fails , the other source will be automatically available for moving the vehicle. The direct connect of the ICE shaft to wheels enables less power transformation and thus achieves higher efficiency. The differential, torque converter and combination of transmission is more efficient than the series HEV's ICE-to-wheel path. Thus, the size of parallel hybrid's electric traction motor is less than what is required in series hybrid. There can be various other combinations and configurations of the two sub-systems as well. However, discussion of these are beyond the scope of this work.

Finally, a series-parallel hybrid is where the vehicle can be powered by gasoline engine alone, the electric motor by itself, or by both. Toyota Prius is configured for a series-parallel drive, as shown in Figure 1. The HEV system is equipped with an electric motor, an ICE and a generator. A power splitting planetary gear is used to integrate these systems which provides the functionality of power flow structure for different modes of operation [4]. There are two kind of motors in this system; the primary electric motor (MG2) is used for providing the mechanical drive power for moving the car through ICE and this (MG2) is also used for recharging the battery during the process if regenerative braking. The secondary electric motor (MG1) is responsible to act as generator which transfer the power from the ICE to recharge battery and also acts as a power source to supply MG2 which assists in propulsion of vehicle [5].

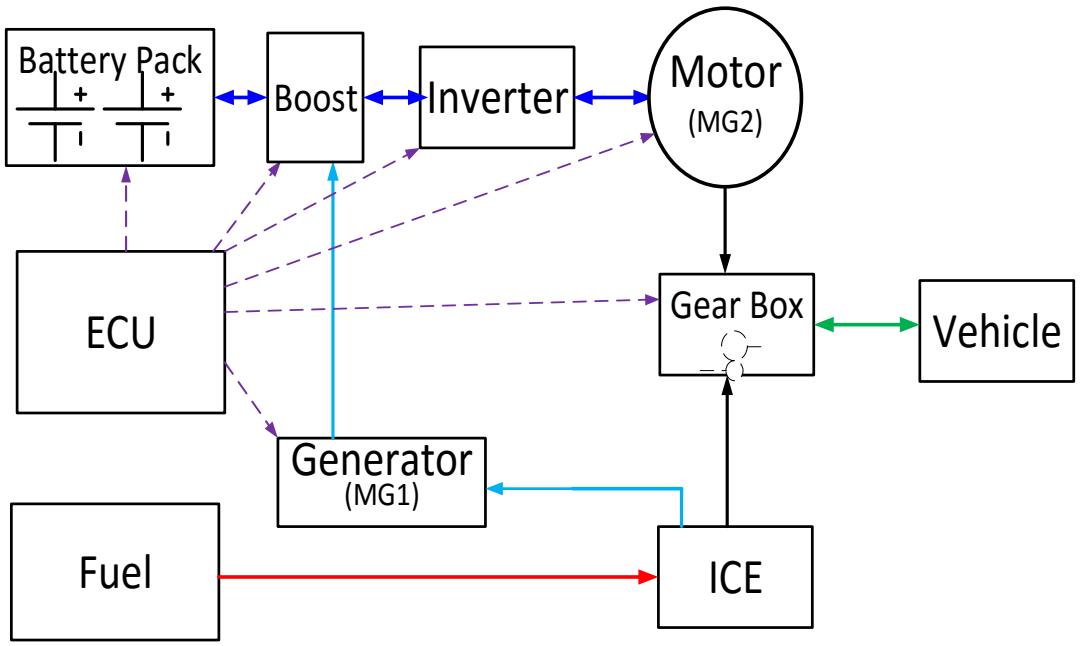

Figure 1 Series-Parallel HEV Drive Block Diagram

HEV's series-parallel combination of electric drive is powered by a battery and a mechanical drive using the legacy ICE engine powered by fuel. The wheels can be driven by ICE engine and electric traction motor. Both systems are connected to the drive shaft of the vehicle, as shown graphically in Figure 2. Both electrical machine and the engine are responsible for producing separate powers that are Ptm and Pice, respectively [6]. The required power produced by the ICE is through the combustion of fuel as the source of power. For the traction motor, the source of power is the battery.

The main idea here is to use electrical drive as long as possible, before the ICE must be used for longer journey, as required, to minimize use of fuel as much as possible. This concept requires the vehicle to use as big a battery as possible. However, due to size and weight limitations, battery is limited in the amount of energy that it can store in the space provided. In order to keep the currents low to minimize I^2R losses in wires, battery is typically designed to be high voltage in the range of 200V to 500V.

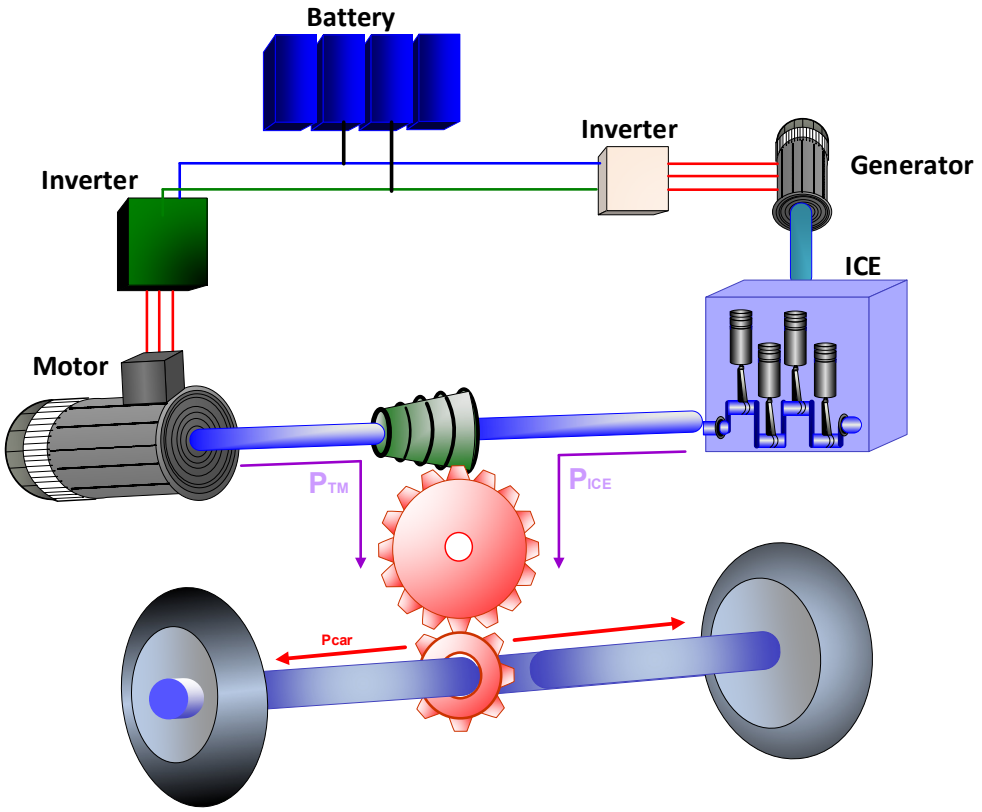

Figure 2 Series-Parallel Hybrid Drive System

Many of the existing HEVs in the market today use either induction motor (IM) or a permanent magnet synchronous motor (PMSM). Size, weight, cost, and efficiency are some of the criteria that are taken into consideration, when doing this evaluation. IM tends to have lower peak power density (50kW/48kg) compared to that of PMSM (50kW/30kg) [7]. However, typically, the PMSM will cost more due to the magnets used in the motor. In the case of Toyota Prius, a PMSM is used as part of the electric drive. Table I, below, shows the main components and ratings of the Toyota Prius electric drive system.

Table I Electric Drive Subsystem Features

Subsystem	Type	Specification
Battery	Nickel-Metal-Hydride	288 V 6.5 Ah
Converter	Boost (IGBT)	600 V 36.5 kW
Inverter	Full H-Bridge w/IGBTs	
Motor	PMSM	300 N (peak)

Although most motors are designed and used to operate at a constant speed and provide constant output, many of the modern systems require variable speeds where electric motors are used. Considerable studies have been done in the areas of variable speed drive (VSD) in order to achieve improvements in efficiency and energy savings. Total electric energy produced in USA is nearly 65% consumed by electric motors. A large percentage of the electric motors in the US are driving fans, pumps, compressors and conveyors where constant speed is desired. Only a small percentage of electric motors are traction devices in automobiles where variable speed is a must. By increasing the efficiency of the mechanical transmission and decreasing the energy input, substantial savings can be achieved to reduce energy consumption. The use of variable-speed drive instead of constant-speed operation can increase the system efficiency from 15 to 27%. The variable-speed drive operation benefits the environment in terms of saving the energy, reduces the atmospheric pollution by lowering the energy consumption and production [8].

With the advent of micro-electronics including processing power, sensors, power MOSFETs, and digital electronics, VSD have taken off. Operating and controlling the motor, inverter, and processing the various sensor signals requires a sophisticated microprocessor based control system. This is typically done using an electronic control unit (ECU), that has CPU and other peripherals built in. A block diagram of a typical CPU based ECU is shown below in Figure 3. All of the proportional integral differential (PID) control as well as signal conditioning and processing is done by the ECU.

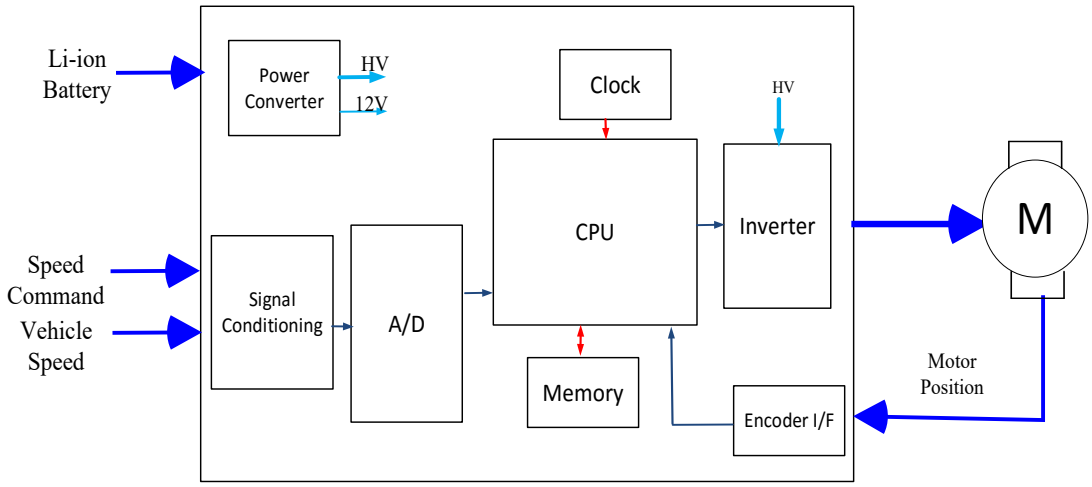

Figure 3 Typical CPU based Electronic Control Unit

The topic of finding fuel efficiency via optimized gear ratios was investigated and published by Minjae Kim et al [9]. The paper described the establishment of the gear ratio while designing the hybrid electric vehicle considering the fuel and battery efficiency. The hybrid algorithm which used Univariate and RSM search method to decide the best gear ratio for hybrid vehicle using less power from the battery. This algorithm successfully achieved reduction of energy up to 0.84%. This proposed algorithm can be used in any vehicle having dual motor tractions [9].

2.1 Electric Drive System

2.1.1 Battery

The high voltage battery is the main power source for the electric motor drive. The battery is sized in its capacity to provide enough energy to last a typical drive period in a day. However, depending on the road conditions and the gradients encountered, the charge may not last that long. Hence, a need to re-charging the battery during the day may arise. It is critical for the control system to operate the vehicle and the motor drive system in the most efficient way possible to ensure highest mileage per battery charge.

In city driving, where the vehicle is constantly required to slow down and stop, it is possible to recover some of the kinetic energy of the vehicle back into electrical energy. This phenomenon is known as regenerative braking, where during deceleration mode, the motor turns into a generator, thus putting charge back into the battery [10].

Rechargeable battery technology involves chemistry and physics. Lithium Ion type battery has emerged as the leading type in most portable devices. However, for larger systems like the automobile, Li-ion is also desirable due to its relatively high energy density. An energy density graph for various battery types is shown in Figure 4 for comparison purposes [11].

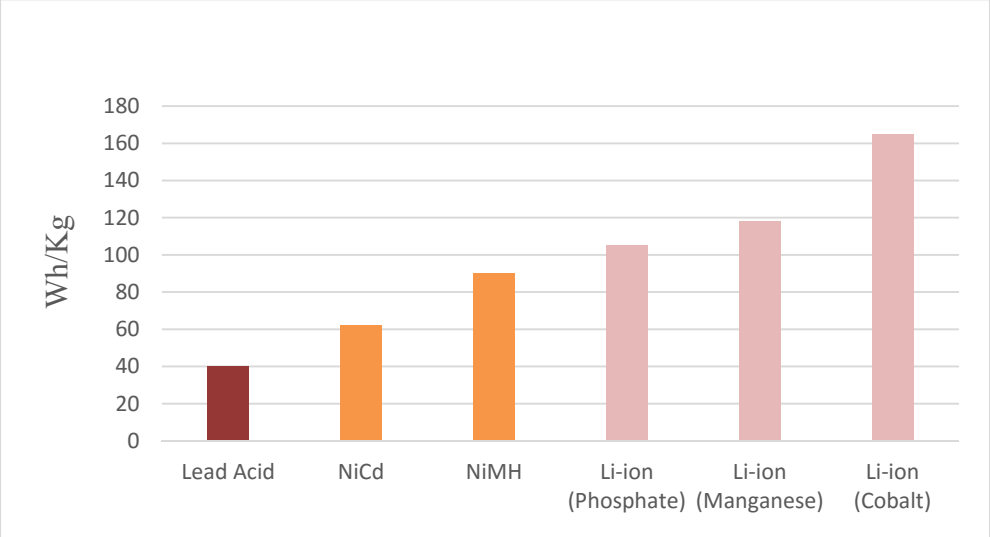

Figure 4 Energy Density of Battery Types

A typical Li-ion cell voltage vs. state of charge (SOC) is shown below in Figure 5. Voltage holds relatively constant (3.2V to 3.6V) across the charge range until it gets close to 0% SOC. Since each cell is only about 3.3V, and rated for about 3000mAh, a battery pack that can power a large system like a vehicle is typically constructed by using cells in series and parallel combinations to provide the proper voltage and total energy. Thus, it would require about 60 cells in series to produce 200V, and about 80 cell in parallel to produce a nominal 50kWh pack.

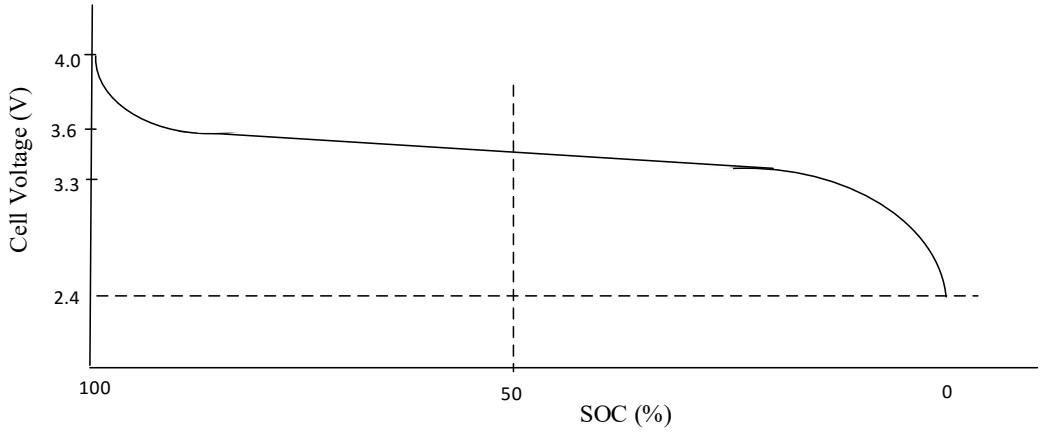

Figure 5 Typical Li-ion Cell Voltage vs SOC

Battery technology is an interesting topic where much of the research is being conducted to improve its performance. For the purpose of this evaluation, an ideal battery source is assumed. This is modeled by using a simple voltage source with zero source impedance. This model can be modified to more closely match the actual battery characteristics. However, modeling of an actual battery pack is beyond the scope of this study.

2.1.2 Motor Drive

2.1.2.1 Inverter

The main function of inverter is to convert the dc voltage to an ac voltage, where the frequency of the drive in synchronous to the motor rotor speed. A power inverter is used to produce a pulse width modulated voltage drive to the motor phases. This in turn allows for controlled currents to flow in the motor windings. Thus the inverter is a major part of the motor drive circuit allowing for controlling the currents in the motor, and motor to produce smooth torque output. A typical inverter drive circuit is shown in Figure 6**.** In this paper, inverter is modeled as an ideal 3 phase current source from the controller.

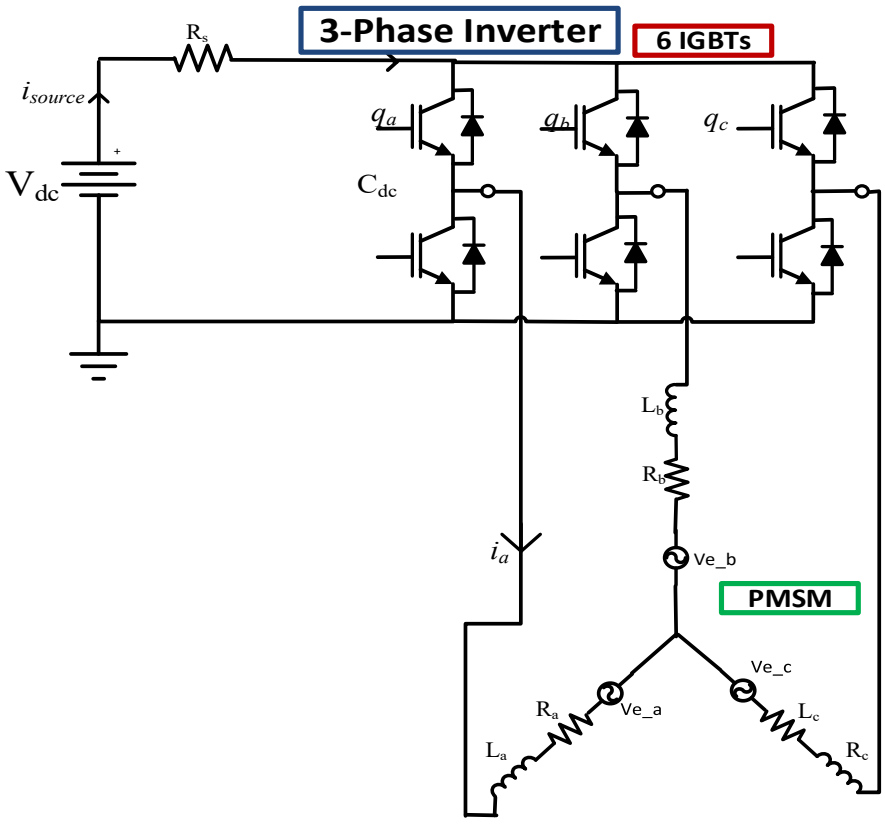

Figure 6 Motor drive model with inverter and reduced order PMSM model

2.1.2.2 Electric Machine

Main function of an electric drive is the ability to convert electrical energy into mechanical energy. This is accomplished by the use of an electric machine or a motor. In this study, a PMSM was used as part of the system modeling. A cross section view of a typical 3 phase, 4 pole PMSM is shown in Figure 7. Surface mounted (permanent) magnets establish the flux in the rotor. The stator windings are in the slots such that a sinusoidal flux density is produced in the air gap.

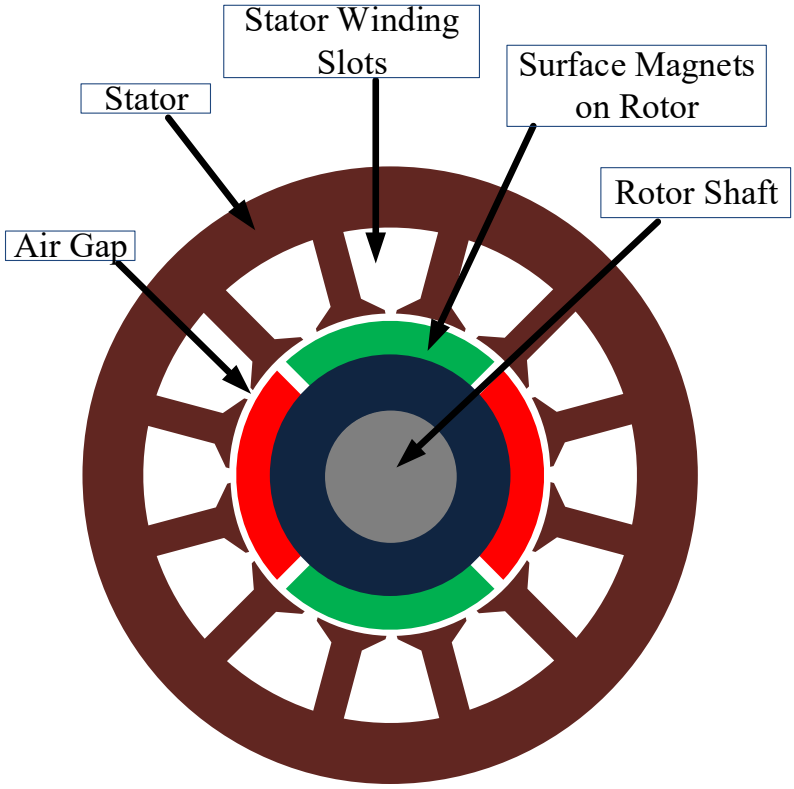

Figure 7 PMSM Motor Cross Section

A typical motor torque and power curve as a function of motor rotational speed is shown in Figure 8. Motor torque as a function of speed is given by

$$\tau = \tau_S - K\frac{1}{\omega_{NL}}\omega, \tag{2.1}$$

where τ_S is the stall torque, ω_{NL} is the no load rotational speed (RPM), and K is a constant.

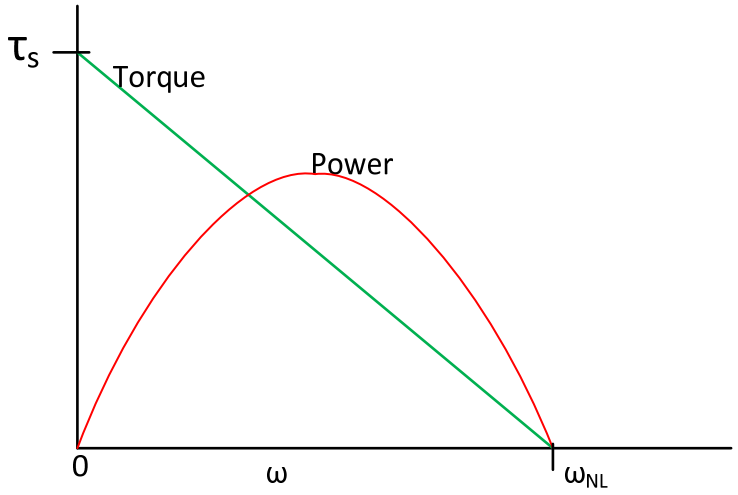

Figure 8 PMSM Torque and Power vs Speed

Motor power as a function of rotational speed, shown in Figure 8, is given by

$$P = \tau\omega. \tag{2.2}$$

A PMSM used in the electric drive can be modeled using the steady state equations. This level of detail is needed for proper analysis and will be used in simulation of the system. Stator voltage equations are defined as

$$v_a = i_a r_a + \frac{d\lambda_a}{\mathrm{dt}} \tag{2.3}$$

$$v_b = i_b r_b + \frac{d\lambda_b}{\mathrm{dt}} \tag{2.4}$$

$$v_c = i_c r_c + \frac{d\lambda_c}{\mathrm{dt}}. \tag{2.5}$$

Flux linkage equations can be written as

$$\lambda_a = L_{aa} i_a + L_{ab} i_b + L_{ac} i_c + \lambda_{ma} \tag{2.6}$$

$$\lambda_b = L_{ab} i_a + L_{bb} i_b + L_{bc} i_c + \lambda_{mb} \tag{2.7}$$

$$\lambda_c = L_{ac} i_a + L_{bc} i_b + L_{cc} i_c + \lambda_{mc} \tag{2.8}$$

where L_{aa}, L_{bb}, and L_{cc} are self-inductances of the stator phases a, b, and c, and L_{ab}, L_{bc}, and L_{ac} are the mutual inductances between the respective phases.

Flux linkages due to the permanent magnets are

$$\lambda_{ma} = \lambda_m \cos(\theta) \tag{2.9}$$

$$\lambda_{mb} = \lambda_m \cos(\theta - 2\pi/3) \tag{2.10}$$

$$\lambda_{mc} = \lambda_m \cos(\theta + 2\pi/3) \tag{2.11}$$

where λ_m is the peak flux linkage due to the permanent magnet, and θ is the rotor position. PMSM motor phases configured as a wye connection is shown in Figure 9.

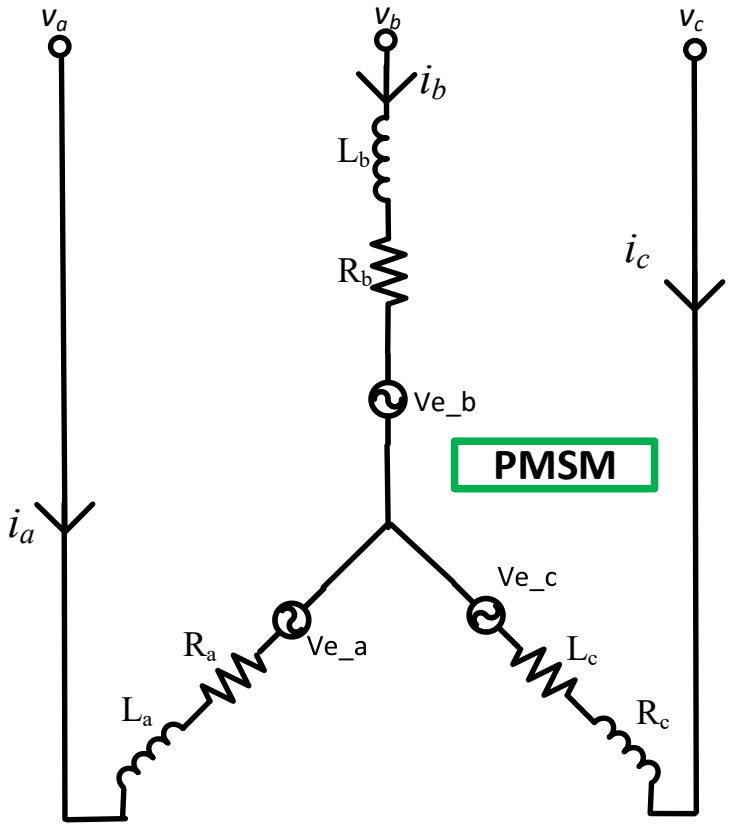

Figure 9 3-Phase PMSM Equivalent Circuit

State equations for the motor phase current are

$$\frac{di_a}{\mathrm{dt}} = \frac{1}{\mathrm{L}}(v_a - i_a Ra - v_{e\_a} - v_n) \tag{2.12}$$

$$\frac{di_b}{\mathrm{dt}} = \frac{1}{\mathrm{L}}(v_b - i_b Rb - v_{e\_b} - v_n) \tag{2.13}$$

$$\frac{di_c}{\mathrm{dt}} = \frac{1}{\mathrm{L}}(v_c - i_c Rc - v_{e\_c} - v_n) \tag{2.14}$$

where, v_a, v_b, and v_c are phase drive voltages, $Ra, Rb,$ and Rc are motor phase resistances, v_{e_a}, v_{e_b}, and v_{e_c} are the phase back-emf voltages and v_n is the neutral point (star point) voltage. Back-emf term increases as a function of motor speed, and varies as a function of rotor position. Back-emf is the artifact of the PMSM due to its generative properties. As the motor spins, the magnets rotating across the stator windings produce a sinusoidal voltage on the windings. This voltage is called the back-emf. The magnitude of the voltage is a function of the rotational frequency.

Due to the fact that torque varies as a function of current and angle, the control system needs to measure the 3 motor phase currents as well as the motor electrical angle. Current needs to be controlled in such a way as to produce the maximum torque achievable at any given angle. This requires a sinusoidal drive signal as a function of the measured angle.

A commonly used technique to achieve this phase alignment and produce the maximum achievable torque is to change the frame of reference from stationary A,B,C frame to what is known as rotational D,Q frame of reference. In fact, this frame transformation, also known as Park's Transformation, converts an (ac) alternating signal into a dc signal for ease of analysis and controls. Another version of this matrix is the power-invariant matrix shown in (2.15). As a result of this (T-matrix) transformation, the signals are separated out automatically into maximum torque producing axis (q-axis) component and 0 (zero) torque producing axis (d-axis) component. The transformed d-axis and q-axis current are

$$\begin{pmatrix} i_d \\ i_q \end{pmatrix} = \frac{2}{3}\begin{pmatrix} cos(\Theta) & cos(\Theta - \frac{2\pi}{3}) & cos(\Theta + \frac{2\pi}{3}) \\ -sin(\Theta) & -sin(\Theta - \frac{2\pi}{3}) & -sin(\Theta + \frac{2\pi}{3}) \end{pmatrix}\begin{pmatrix} i_A(\Theta) \\ i_B(\Theta) \\ i_C(\Theta) \end{pmatrix} . \tag{2.15}$$

Since d-axis produces no torque, ideally, the measured and controlled d-axis current should be 0. Also, since q-axis is the maximum torque producing axis, the q-axis current should be the actual commanded current.

A complete system block diagram of the model is shown in Figure 10.

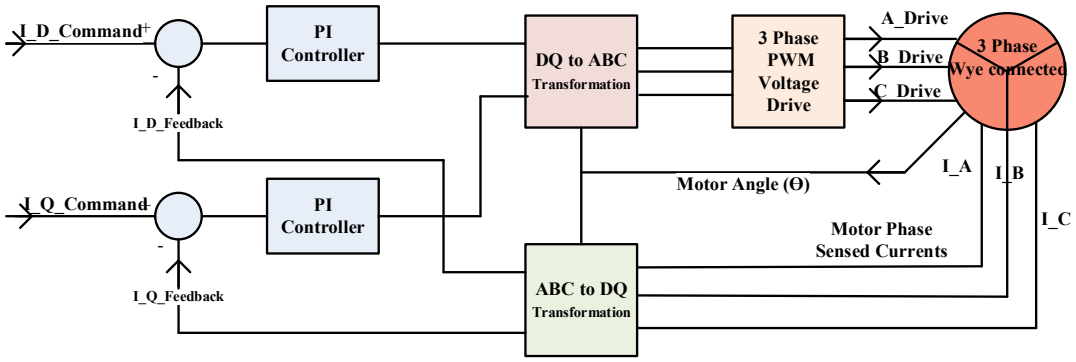

Figure 10 Block Diagram: Closed Loop Current Control

This topology employs a closed loop current control method utilizing a PI controller. An independent d-axis and q-axis command is applied and controlled in order to minimize the q-axis current, and to control the q-axis current to the desired value to produce torque. Also evident from this block diagram is that an inverse transformation is necessary to convert the DQ voltage commands back to the ABC reference from in order to drive the 3 motor phase voltages. The phase voltage in the ABC reference, using the inverse transformation, are given as

$$\begin{pmatrix} v_A(\Theta) \\ v_B(\Theta) \\ v_C(\Theta) \end{pmatrix} = \begin{pmatrix} cos(\Theta & -sin(\Theta) \\ cos(\Theta - \frac{2\pi}{3}) & -sin(\Theta - \frac{2\pi}{3}) \\ cos(\Theta + \frac{2\pi}{3}) & -sin(\Theta + \frac{2\pi}{3}) \end{pmatrix} \begin{pmatrix} v_D \\ v_Q \end{pmatrix}. \tag{2.16}$$

This inverse transformation back to the ABC reference frame allows the loop to be closed so that the 3 phase drive voltages can reach the desired levels to produce phase currents. For the purpose of this analysis, motor saturation and other non-linear effects are ignored. From conversion of the phase currents to the d-q rotating from stationary frame, the dynamic state equations can be written as

$$\frac{di_d}{\mathrm{dt}} = \frac{1}{L_d}(v_d - i_d R_s + \omega_m L_q i_q), \tag{2.17}$$

$$\frac{di_q}{\mathrm{dt}} = \frac{1}{L_q}(v_q - i_q R_s - \omega_m L_d i_d - \omega_m \lambda_m), \tag{2.18}$$

and the motor torque can be calculated as

$$T_e = (\frac{3}{2})(\frac{P}{2})(\lambda_m i_q + (L_d - L_q) i_q i_d) \tag{2.19}$$

where P is the number of poles in the machine. In this case, a 2 pole (P=2) motor is used in the modeling.

The equivalent circuits for the above equations are shown in Figure 11 below [12].

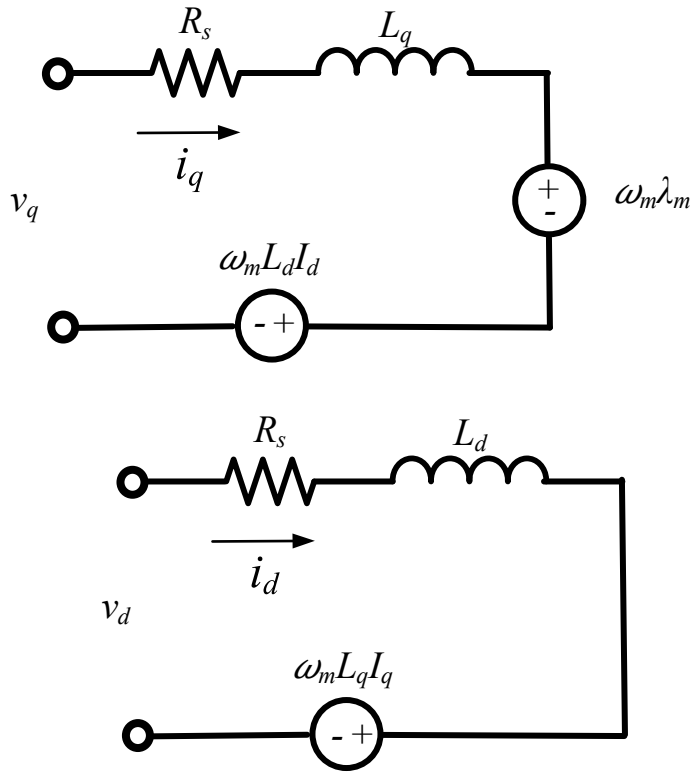

Figure 11 Equivalent Circuit for PMSM in d-q frame

2.2 Vehicle Load Model

Vehicle load can be a function of multiple variables, including aerodynamics. Here, we take into account the parameters that provide the largest effects on the vehicle in terms of

load. Vehicle load model equations are below. Accelerating mass of vehicle will be the force on the wheels. Wheel force is then calculated as

$$f_{wheel} = M_T \frac{dv}{\mathrm{dt}} \tag{2.20}$$

where *v* is the velocity of the vehicle, and M_T is the total mass calculated as $M_T = M_{veh} + M_{tire}$. The torque on wheels can be determined as

$$T_{wheel} = r f_{wheel} = r\, M_T\, \frac{dv}{\mathrm{dt}} = r\, M_T\, \frac{d(r\omega_{wheel})}{\mathrm{dt}}$$

$$= r^2\, \frac{d(\omega_{wheel})}{\mathrm{dt}}, \tag{2.21}$$

where r is the radius of the wheels, and ω_{wheel} is the rotational speed of the wheel.

Rolling resistance of tire is given by

$$f_{rr} = \mu_{rr}\, M\mathrm{g}, \tag{2.22}$$

where μ_{rr} = rolling resistance coefficient and g = 9.81 $\frac{m}{s^2}$. Viscous drag is given by

$$f_d = \frac{1}{2} \rho\, A\, C_d\, v^2 \tag{2.23}$$

where air density ρ = 1.2 $\frac{kg}{m^3}$, *A* is the cross sectional area, and C_d is the viscous drag coefficient. Force due to slope effect is determined as $f_{slope} = M\, g\, sin(\theta)$, where θ is the angle of the slope. For small slopes, the force can be approximated as $f_{slope} = Mgslope$, where gravitational acceleration g = 9.81 $\frac{m}{s^2}$. Force due to bearing friction is given by $f_{bear} = \frac{k_b}{r}\, \omega$. Thus, total force can be calculated as

$$F_T = f_{wheel} + f_{rr} + f_d + f_{slope} + f_{bear}. \tag{2.24}$$

Load torque can be then determined by $T_L = F_T\, r$, where r is the radius of the tire.

Finally the vehicle tire rotational equation is given as

$$\frac{d\omega}{dt} = \frac{T_e - T_{\mathrm{LOAD}}}{J} \tag{2.25}$$

where J, in Kg·m^2, is the moment of inertia, Te, in Nm, is the torque driven from the motor, and ω is the tire rotational speed of the tires in rad/s.

2.3 Power Balance and Energy Conservation

The three components to the power calculation are input power from the battery, motor output power, and vehicle load power. Input power from the battery source can be calculated as

$$P_i = v_a i_a + v_b i_b + v_c i_c. \tag{2.26}$$

In the d-q frame of reference using Park's transformation, this equation becomes

$$P_i = \left(\frac{3}{2}\right)(v_d i_d + v_q i_q). \tag{2.27}$$

Motor output power is simply calculated as a function of torque and motor speed as

$$P_{mo} = \tau_m \omega_m. \tag{2.28}$$

Vehicle output power can be calculated using velocity and total force as

$$P_v = V_s F_T. \tag{2.29}$$

For a system that does not store energy, the electrical power from the battery source must be the sum of the mechanical power output and the system losses. If a lossless motor model is assumed as a first order, then the motor power will be equal to the vehicle output power. This is used in the simulation to ensure that the model is designed properly and that the obtained results are correct.

For the battery, however, it is the energy usage that is of importance. The energy used from battery can be calculated from power as $E_b = \int_0^t P dt$. The main intent of this study is to minimize the usage of energy from the battery by using the most optimum gear ratios for motor drive. Simulation results will show that gear ratio selection has a significant effect on the amount of energy used during a city drive cycle.

2.4 Gear Box

Since the motor is designed to operate most efficiently at higher speeds, a gear ratio is typically required to drive the wheels of the vehicle, which run a much lower speeds than the motor. The problem which arises in the case of hybrid powertrain configuration is to find the best gear ratios and arrangement which can cover more mileage with the lowest use of electricity from the battery. The problem of minimizing the fuel consumption depends upon several factors which are gear ratio, torque of the engine over the entire cycle. If appropriate gear ratios are selected, energy minima can be found thus leading to highest possible mileage [13]. An example of the gear box for power transmission is shown in Figure 12.

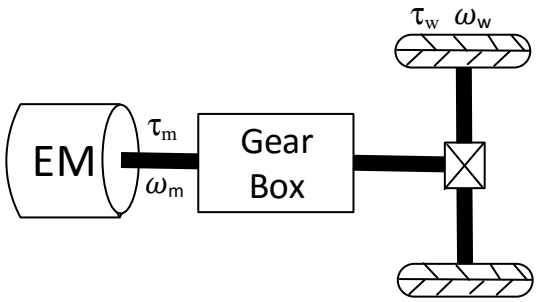

Figure 12 Motor to Wheel drive with Gear Box

The gear reduction allows the axle to spin at a lower rate, and increase the torque, yet receive full power from the motor drive. Since the motor can spin at a high rate, the gear ratio allows the motor to be at the low torque. This can be shown mathematically as

$$P = \tau_m \omega_m = \tau_w \omega_w = \tau_w (\frac{\omega_m}{G}) \tag{2.30}$$

where ω_w is the wheel speed, τ_w is the torque at the wheel and G is the gear ratio. Most EVs currently use 1 to 2 gears to maximize the motor efficiency, however, many hybrids use no gear at all. This model does work, but does not allow for smaller more efficient motor to be used.

A design study of independently controlled transmission was done with objective to find the planetary gear configurations with respect to different speed ratios within a given range.

Speed ratio can be defined as ratio between input engine speed and the output speed of the vehicle. By changing the connections among the planetary gear, many possibilities can arise in terms of achieving the efficiency of the vehicle [14].

Another practical study of stochastic method was used in which the driving cycle was approximated using the Markov chain instead of prior knowledge. This method was applied to a parallel hybrid power train and the results shows a significant amount of reduction in the usage of electricity from the battery [15]. The inputs which were varied were the gear ratios and the power distribution. Different gear ratios were used which showed that selecting the best combination of the gear ratio can reduce the usage of electricity from the battery and can produce improved mileage.

The above literature review shows that the selection of proper gear ratio can be useful in efficiently utilizing the power of the drive, and minimizing the energy consumption from the power source [16]. Through simulations of the traction drive using city drive cycle, the optimum gear ratios can be determined. The goal of the next phase is to show that gear ratios can be used to alow for smaller high speed motor. Also, optimizing the gear ratios can be beneficial to saving power during jouney, thus getting more mileage from the single battery charge.

3 MATLAB/Simulink Modeling

3.1 System Modeling

A system based model was developed based on the theoretical calculations shown earlier. The five main parts to the overall model are motor model, vehicle model, gear box model, control block model, and power balance and energy calculations. Complete high level model of the system is shown below in Figure 13. Four main blocks that were developed as part of the overall model are control, motor model, gear box and vehicle load model. Details of these blocks are discussed in the subsequent sections. Power-energy block is simply used to calculate and store the input and output power and energy values during the drive cycle.

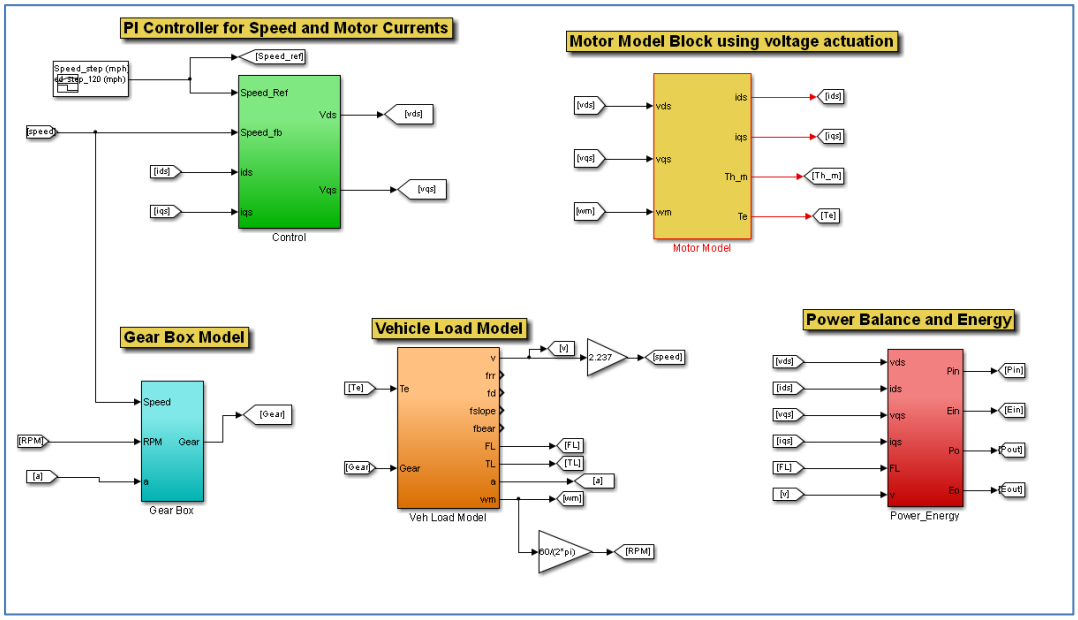

Figure 13 System Model Block Diagram

3.2 Motor Modeling

A PMSM motor model was developed based on the state equations in d-q reference frame. This allows for easier control of the currents. The model uses the Park's transformed variables in d-q reference frame. Motor model is shown below in

Figure 14. Model developed here in Simulink is based on the state (2.17), (2.18) and (2.19). These equations can be modeled using the blocks such as integrator, summing junction, multipliers, and dividers, to represent the full state equation. As an example, i_{ds} is the state output, L_d, L_q, and R_s are motor parameters which are constants, and v_{ds} and i_{qs} are inputs.

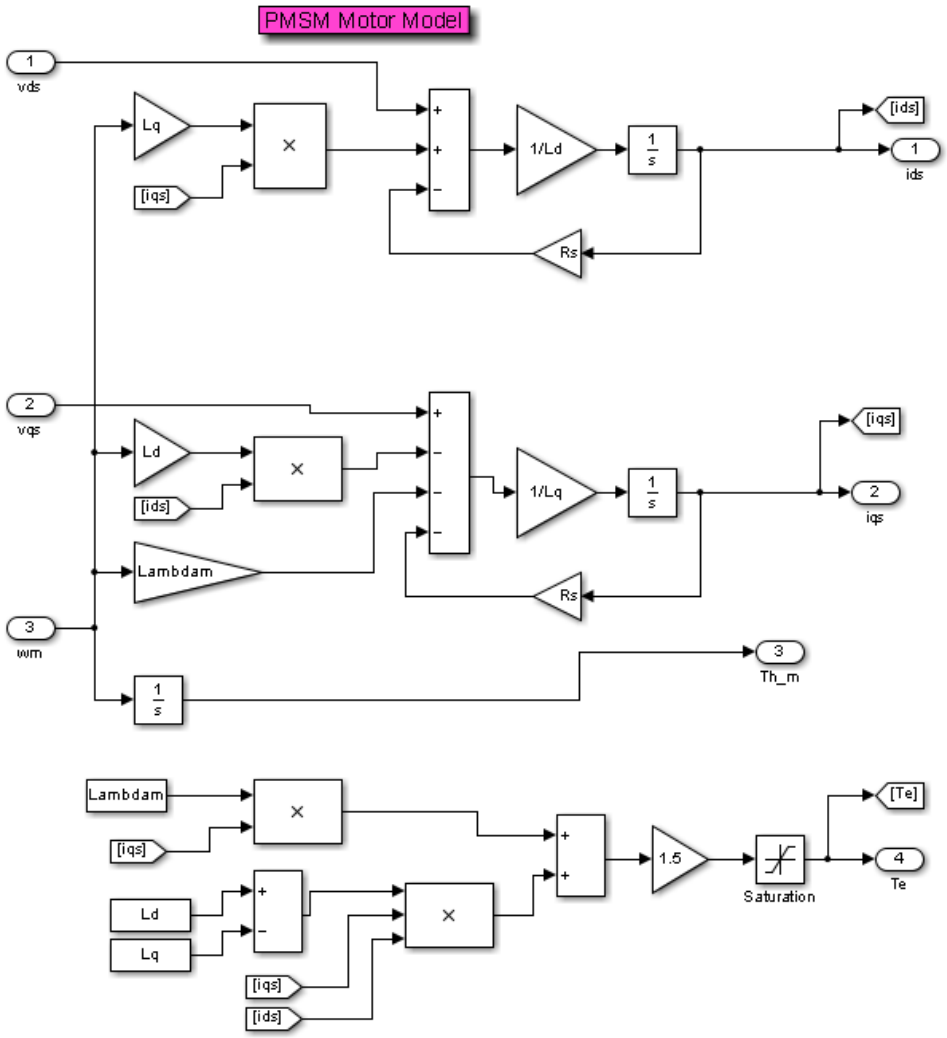

Figure 14 PMSM Motor Model

3.3 Control Modeling

Proportional integral differentiator (PID) type controllers are quite common in the industry. This model uses a simple PI based control loop for vehicle speed control. Also, the q-axis current can be controlled in the same loop. The d-axis current is controlled to zero "0" amps, since only the q axis current produces torque. The gains, Kp and Ki, were chosen to provide a critically damped response to a step input, as well as a reasonable steady state

error of less than 2%. This model consists of amplifiers, inverters and all other important functions which are used in the control systems to check the stability and characteristic of the model.

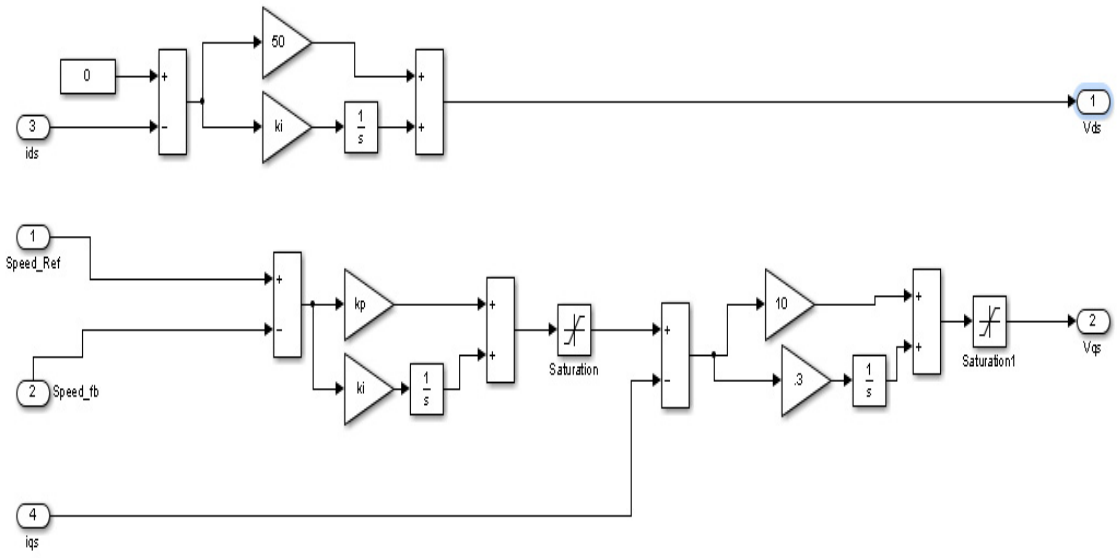

Figure 15 PI Controller for Speed and Current

3.4 Gear Modeling

The main objective of the simulation is to find the combination of gear ratios that produce the most energy efficient drive cycle, and provide the highest possible mileage. For the baseline model, nominal gear ratios were chosen such that sufficient torque can be produced by the drive train to propel the vehicle, and the sufficient power can be generated and delivered to the wheels. In order to find the optimized gear ratio for lowest energy consumption, a range for each gear was used. The range of the gears was chosen to ensure that vehicle can produce reasonable torque and power to propel the vehicle during the drive cycle load conditions. Simulation was setup to use random integers within the range for each gear, and determine the energy used during the drive cycle.

Table II Gear Ratios

Gear	Nominal Ratio	Ratio Simulation Range
G1	16	9 - 20
G2	8	4 - 15
G3	5	2 - 7
G4	3	1 - 4

A state machine model for this gear transitions used in the simulation is shown in Figure 16. Here we use the model to ensure that the motor speed does not go well above its rated speed of 5000RPM. The model allows for both up-shifting during acceleration conditions and down-shifting during deceleration.

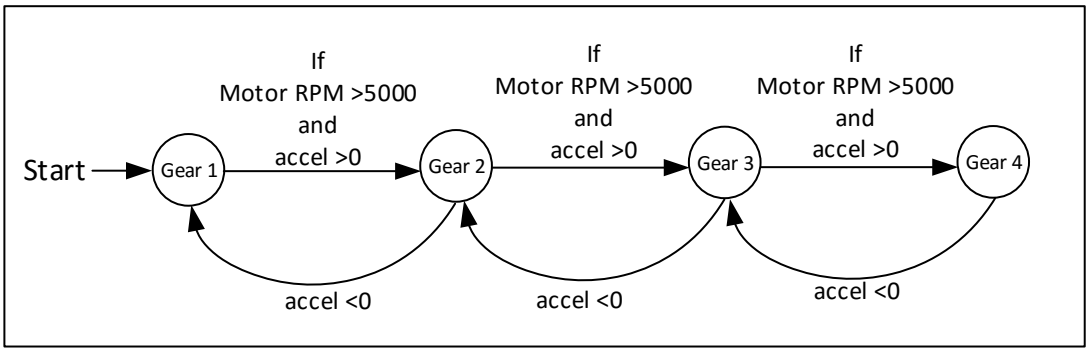

Figure 16 Gear transition state machine

3.5 Load Modeling

A vehicle load model was developed based on key vehicle parameters and environmental conditions. Vehicle weight of 1500 Kg was used based on passenger car fleet averages published by the National Highway Traffic Safety Administration (NHTSA). Some of the other key parameters are listed in Table III. Although viscous drag coefficient is a function of the aerodynamics of the vehicle, an average value of 0.5 was used. Many of the older

model cars would have higher value between 0.6 and 0.9, and the newer cars due to better frontal shapes would have values in the range of 0.25 to 0.4. Complete vehicle load model developed in Simulink and shown in Figure 17, is based on the equations developed in section 2.2.

Table III Load Model Parameters

Parameter	Value	Unit
Vehicle weight	1500	Kg
Tires and Rotating Parts	50	Kg
A_{Front}	3.7	m^2
C_d	0.5	
r_{tire}	0.3	m
Tire loss coefficient	0.01	

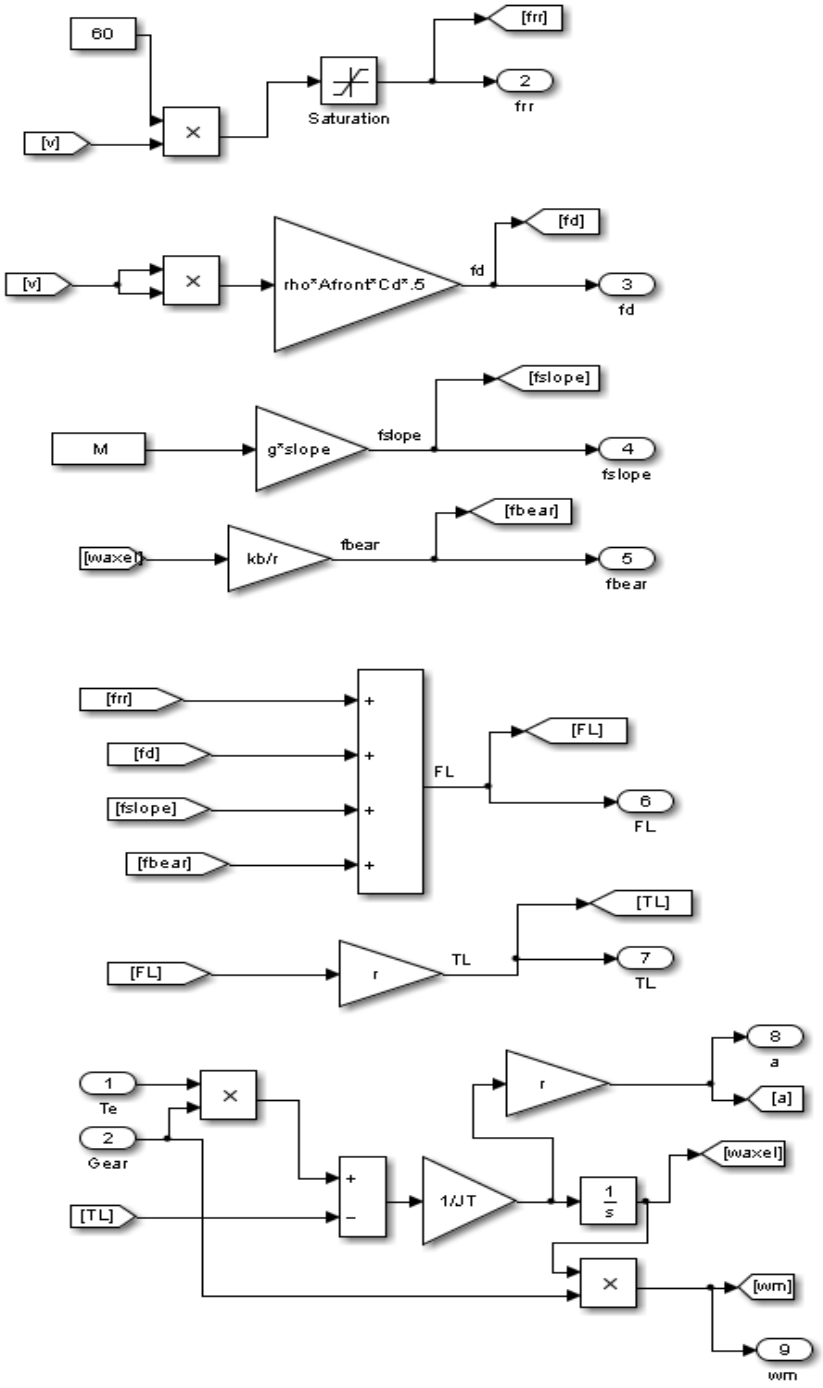

Figure 17 Vehicle Load Model

3.6 Road drive cycle models as inputs

Two types of speed inputs as reference were used for simulation. First, the step input for the vehicle speed is used to ensure that the model is behaving as expected, and that its' response is accurate and stable. Second, Urban Dynamometer Driving Schedule (UDDS), is used as the basis to assess the overall system performance for energy efficiency [17]. UDDS is typically used by the EPA as a reference driving profile for testing of fuel economy for light vehicles.

To understand the behavior of the system model and controls, a step input was used. This allows for debugging of the model as well as fine tuning of the parameters to ensure that the output behaves as expected. A step of 70 MPH was used as a speed input for this test case to show the system response.

For the performance evaluation of the vehicles the automotive industry and governmental agencies perform standard tests which are called standard drive cycles on the basis of which certification of vehicle fuel economy is given. The functionality of standard drive cycles are such that they have both the road grade and speed components.

One of the commonly used standard test is UDDS in which the drive cycle covers a distance of 7.5 mile in 1369 second with average speed of 19.6 mile per hour. In this 7.5 miles covered, the vehicle has frequent stops and starts. This parameter was also taken as input for the simulation. The Figure 18 shows the time-dependent velocity profile. Every vehicle must function according to the following graph. These are the transient drive cycles in which there is a lot of change in the speed due to on-road driving conditions.

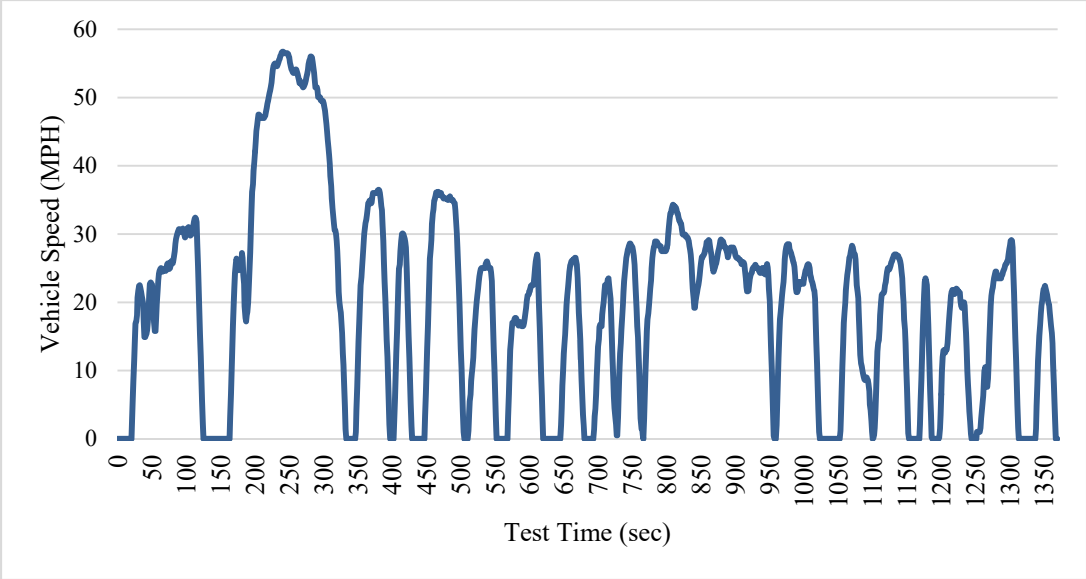

Figure 18 Velocity-time UDDS Graph

The graph shows the vehicle speed with respect to time. These are the standard drive cycles which each vehicle must be tested with. The model presented in this thesis was simulated with this UDDS drive cycle.

4 Simulation Results

4.1 Speed and Torque Results for Step Input

One of the best ways to test a control system is to input a step function. Understanding the system response to a step input is important in order to determine how well the system is designed and tuned. It provides response in two ways – the transient response and the steady state response.

In this simulation, vehicle speed was used as a step input not only to determine the system parameters in setting PID loop, but also to initially optimize the gear ratios. Step response of the system is shown in Figure 19. Step response shows the settling time and the steady state error of the system control loop. Settling time shows how much time it takes for the vehicle to achieve desired speed. In below figure, settling time is shown to be 20 second, achieving steady state commanded input in this duration. Initially the torque produced by the motor is high due to low speed. Acceleration increases initially since the vehicle starts from zero speed. As the speed reaches steady state, the acceleration decreases to zero. This simulation also shows that the resulting vehicle speed reached the desired reference speed, with low error, and no observable overshoot. As discussed earlier, this is important in confirming that the PI gains have been selected correctly.

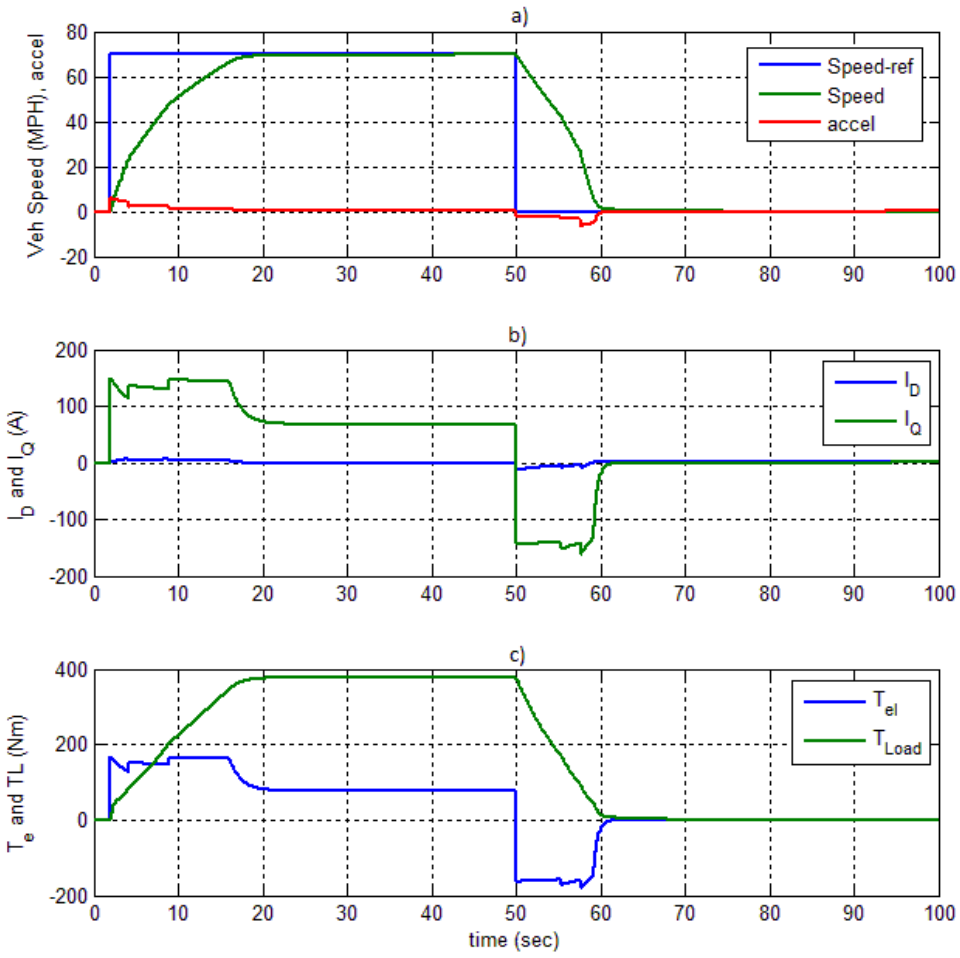

Figure 19 Step Response of System
a) Vehicle speed, b) Motor Current, c) Torque

The Figure 20 shows the power and energy profile when step input is used as input. Initially the input power drawn from the battery is high that is due to initial high load requirement, mainly due to the acceleration required. Motor has to provide power to overcome this force and equally proportional power is drawn from the battery. As the vehicle speed reaches steady state, acceleration becomes zero and input, output power become theoretically equal. Similar response is observed in case of Energy input and output. Maximum power output delivered is about 40 kW for this case.

During the time when the set input speed is zero, and the system goes into what is known as regenerative braking mode. Here, the mechanical system is putting power back into the battery during this time as the vehicle [17] decelerates, and the speed goes down to zero. This can be clearly seen in the plot as the negative input power.

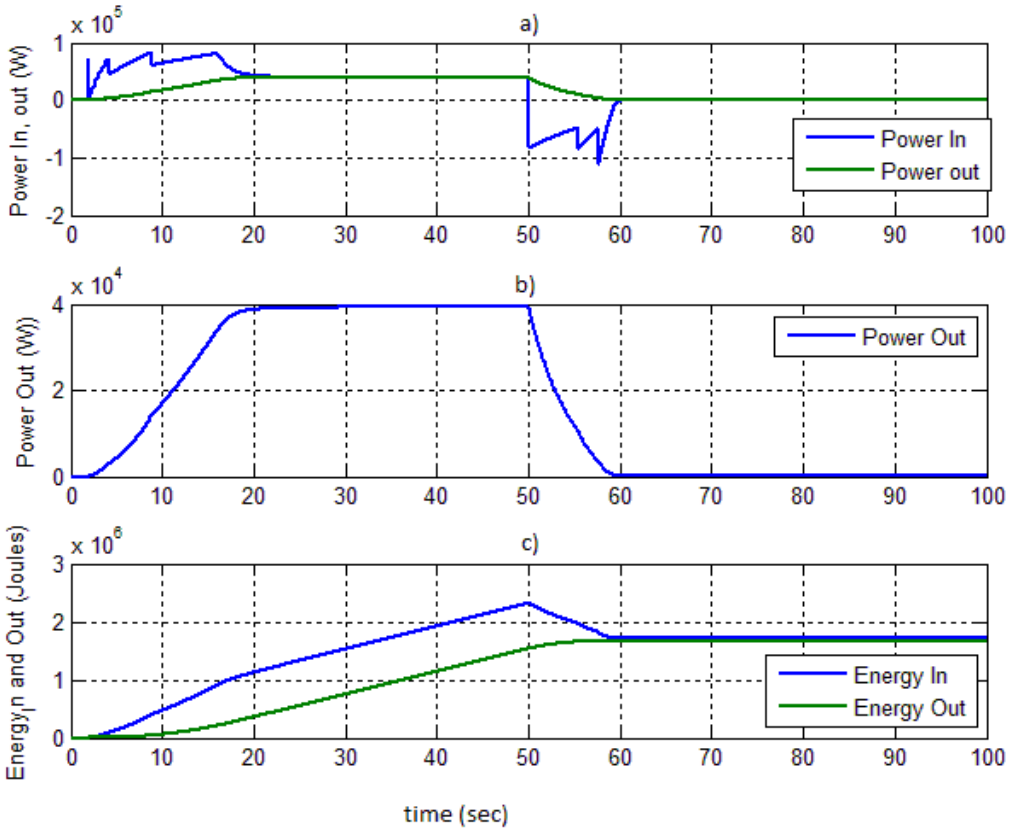

Figure 20 Step Response of system
a) Power In, Power out, b) Power out zoomed in, c) Energy In, Energy out

The results obtained when step unit function is used as input are according to the control system. The system is performing well when step input is given.

A more in depth analysis of the effect of gear ratios on the wheel torque and wheel power is then conducted. Results of this analysis are shown in Figure 21. This graph clearly shows that vehicle can provide a high traction effort in 1st gear. The vehicle also maintains a reasonable top speed in 4th gear. This matches well with the time simulation shown

earlier, with the 70 MPH commanded speed. The vehicle reached and stayed in 3rd gear in steady state. Although, only 40 kW power was required during steady state at 70 MPH, this traction drive is capable of up to 90 kW power.

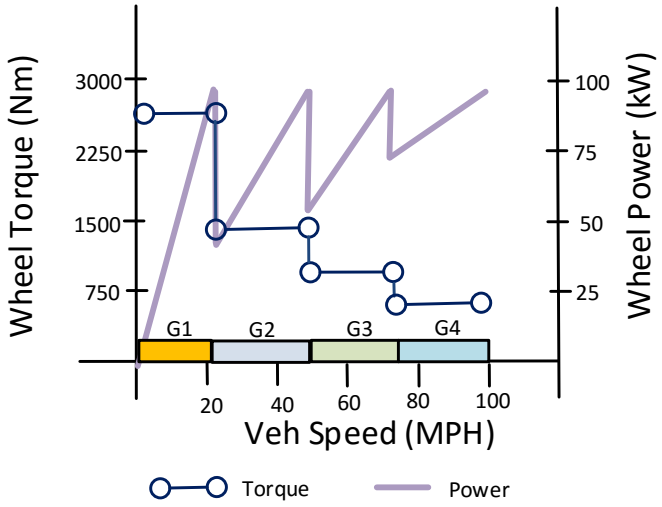

Figure 21 Vehicle Traction with 4-Speed Transmission

4.2 Simulation Results using UDDS

In this part of the simulation, UDDS is applied as an input and the results are captured. The characteristics of these standard cycles have been explained in section 3.52. Every vehicle must function per the characteristics of the UDDS standard graph in passing EPA standards. These are the transient drive cycles in which there is a lot of change in the speed due to on-road driving conditions. The following are the results achieved after the simulation. The speed of the vehicle was controlled according to the UDDS reference speed which can be seen in Figure 22. The model performed as expected as can be seen in the graph. Output speed closely follows the set input speed with very low steady state error and good response time.

The torque is also shown in the Figure 22. The graph shows that at the points where the hybrid electric vehicle is decelerating the Torque in the graph goes negative. This graph

shows that the control system is working correctly and the requested torque is properly achieved in the proposed model.

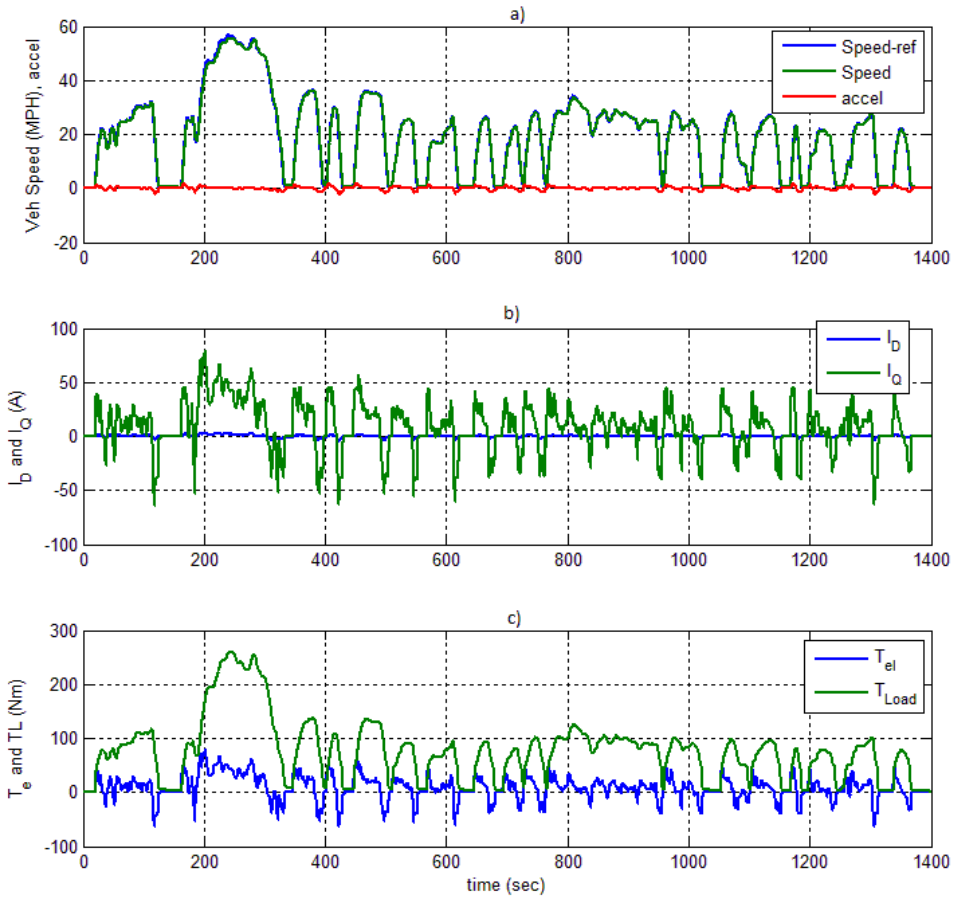

Figure 22 System Response with UDDS
a) Vehicle speed, b) Currents, c) Motor torque and Load torque

The Figure 23 shows the power and energy profile of the HEV. The output power is the power which is given to the wheel and the input power is the power which is drawn from the battery. The figure also shows that there is variation in input power as it is some times in the negative acting as a generator and some times in the positive supplying the power to the vehicle which is the case according to the control systems. The points in the graph where the speed is approaching zero shows again the behavior during regenerative braking

and re-capturing of some of the energy during this time period. The energy which is supplied to the vehicle is fully utilized in terms of power balance. The power system works as defined per the UDDS cycle.

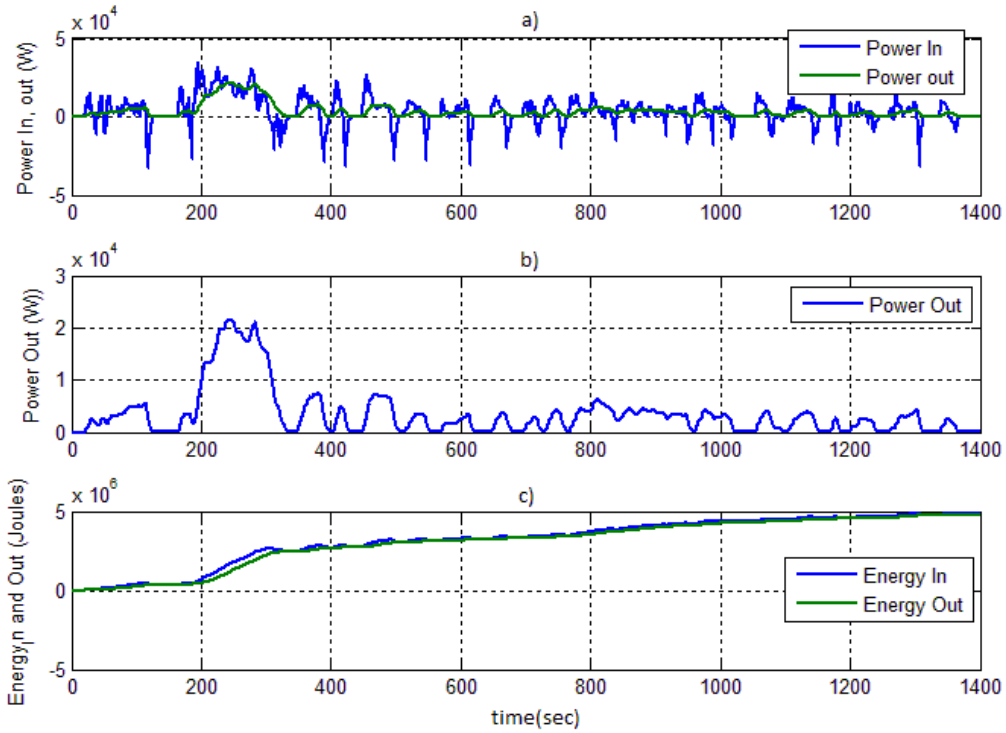

Figure 23 System Response with UDDS
a) Power In, Power out, b) Power out zoomed in, c) Energy In, Energy out

4.3 Optimization of Gear Ratios

As discussed in section 3.4, simulation was setup to run random ratios for each gear within the specified range. A total of 200 (50 for each gear) test cases were run. The final energy usage values were stored for each case of gear ratios. This 200 case simulation allows us to determine the best gear ratios to minimize the use of energy. Results were captured for each run and plotted to show the ENERGYIN and ENERGYOUT as a function of gear ratios. The minima of the input energy from the battery can be determined by the use of the combination of different gear ratio. The simulation results are shown for both the Step

Input, and the UDDS cycle, in the following figures. The results shows effectiveness of the proposed method which stated that different combination of gears can play an important role in determining the energy usage efficiency from the battery.

Figure 24 and Figure 25 shows the graph for results of Step Input. Figure 24 shows ENERGYIN, which is the energy from the source (battery) as a function of cases for gear ratio combinations. Figure 25 shows the different combinations of Gears for G1, G2, and G3 and G4. The data is also sorted in the order of smallest value of ENERGYIN to the largest value.

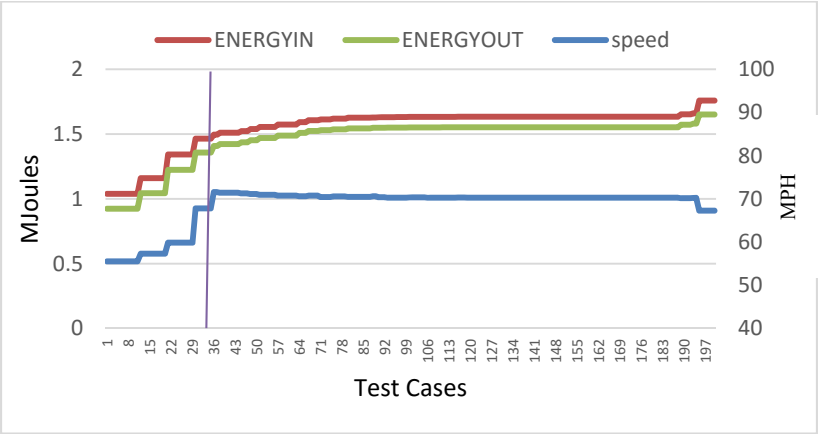

Figure 24 Sorted Test Cases with Step Input
for Energy In (ENERGYIN), Energy Out (ENERGY OUT)

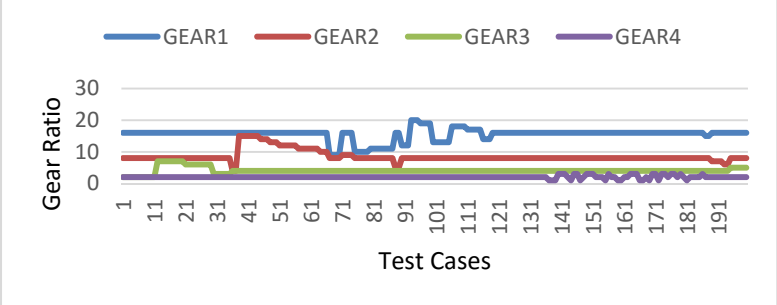

Figure 25 Gear Ratio combination vs. Test Cases with Step Input

This step input case was run as a quick check to determine the effects of the gear ratios on the energy consumed. Only one gear was changed randomly, while, other were held constant at nominal values. The minimum energy in the graph drawn from the battery is about 1 MJoules. However, the speed, for this case, did not reach the desired reference point. This shows that not all possible combinations will work to produce the proper torque for the vehicle to operate under harsh demands. The main hypothesis, however, is proved, in that the energy consumption varies significantly as a function of gear ratios. If the combination of gear ratio is not properly used the input energy can increase and the drive system will not operate at its most efficient point.

A similar separate simulation was run with the input of UDDS drive cycle. This simulation was intended to find the actual energy used during the UDDS drive cycle while all gear ratio combinations were randomly selected within their ranges. Results of the UDDS based simulation are shown in Figure 26. Energy is plotted as a function of gear set combination. The results are sorted and shown with the ENERGYIN increasing from low to high. The selection of appropriate gear ratio has very important effect on the input energy. This shows that the best gear ratio combination can be chosen in order to minimize the energy usage from the battery.

Results of this simulation show that the gear ratio selection is a very powerful mechanism as part of EV drive system to maximize the performance. Based on the UDDS multi-case simulation, it is observed that the energy consumption from the source can vary from a low of 4.95 MJoules to a high of 5.55 MJoules, an increase of 12%. This is a significant energy savings for the vehicle during a UDDS type journey, as more commuters are now choosing to use EVs and HEVs for city driving.

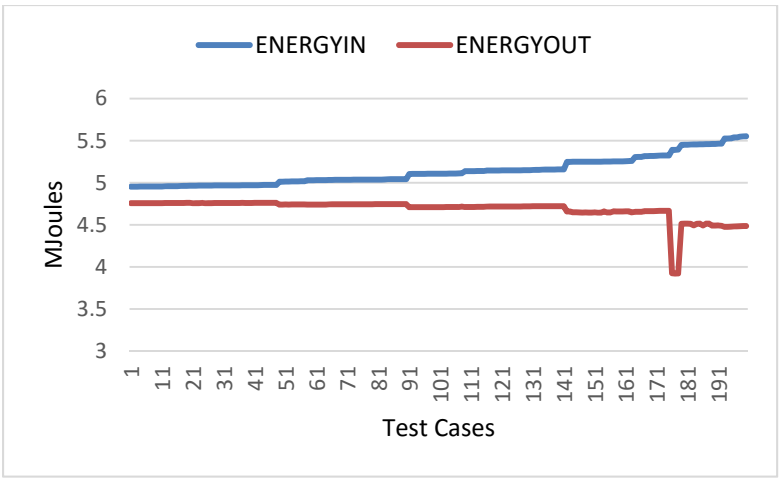

Figure 26 Sorted Test Cases with UDDS
for Energy In (ENERGYIN), Energy Out (ENERGY OUT)

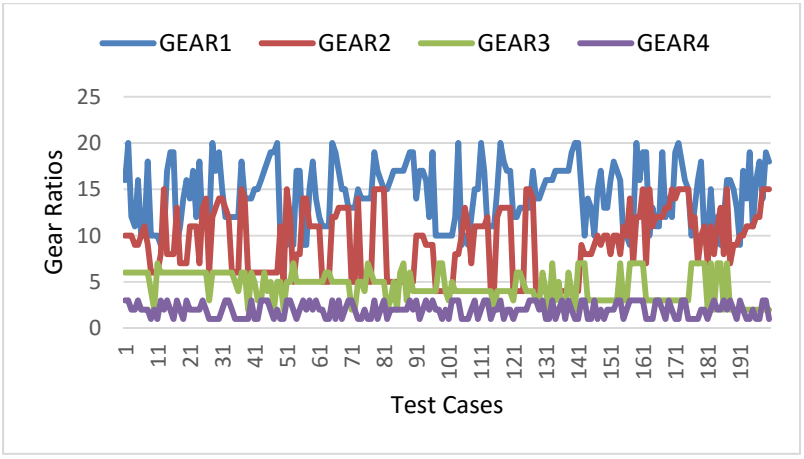

Figure 27 Gear Ratios vs. Test Cases with UDDS

5 Conclusion

This project paper describes the development of a traction drive and vehicle load model for an HEV including a gear set model that allows for determining the optimal gear set combination to achieve the lower energy consumption from a HV battery. A detailed model of PMSM and vehicle load was developed in MATLAB/Simulink. Each stage of the model was separately simulated to ensure that the dynamic and steady state behavior was as expected. Motor and drive parameters were chosen to be close to the 2010 Toyota Prius system, which is documented in a report published by US Department of Energy. A 4-speed gear switching mechanism was modeled using a Simulink state machine transition table to ensure proper operation in both up-shifting (during acceleration) and down-shifting (during deceleration).

Results were very satisfactory in terms showing how various gear ratios can be tested and then evaluated for optimum points to minimize energy loss which is the achievement in the proposed model. Maximizing the mileage from a battery is just one application where this technique can be used very effectively. System performance can be fine-tuned, as well as optimized for longer journey and conserving the battery charge. However, this method does require a broader range of gear ratio to be used for this optimization. Automatic transmission can be used to program the shift points to the exact values required.

6 Areas of Further Research

To further improve this model, there are several areas that can be considered. One major area that would greatly enhance this model is the do further optimization to capture the regenerative braking energy. Switching points of down-shifting can be optimized to yield the highest recapture of the energy during braking.

The system model was based on ideal motor and power electronics. However, these subsystems can also be modeled to more accurately reflect the physical components. Magnetic saturation and other non-linear effects can be taken into account to make the model more realistic.

Other areas that can be further developed to be more realistic would be the battery, the dc-dc converter as voltage booster, and the inverter. These components also add multiple non-linear effects and were beyond the scope of this project. However, in order to get more accurate results for the energy optimization, these models can be taken into account. Actual components used to realize these sub-systems (inductors, power MOSFETs. IGBTs, etc.) can add complexities to modeling and simulation, but may provide other insights into the behavior of the overall simulation.

7 References

[1] D. Doerffel and S. A. Sharkh, "System Modeling and Simulation as a Tool for Developing a Vision for Future Hybrid Electric Vehicle Drivetrain Configurations," in *IEEE Vehicle Power and Propulsion Conference*, pp. 1 - 6, September 2006.

[2] M. Olszewski, "Evaluation of the 2010 Toyota Prius Hybrid Synergy Drive System," U.S. Department of Energy, Washington, D.C., 2011.

[3] P. Mishra, S. Saha and H. Ikkurti, "Selection of Propulsion Motor and Suitable Gear Ratio for Driving Electric Vehicle on Indian City Roads," *International Conference on Energy Efficient Technologies for Sustainability,* pp. 692-698, April 2013.

[4] M. Bertoluzzo, P. Bolognesi and G. Buja, "Role and Technology of the Power Split Apparatus in Hybrid Electric Vehicles," in *The 33rd Annual Conference of the IEEE Industrial Electronics Society*, Taipei, pp. 256 - 261, November 2007.

[5] A. E. Bayrak, Y. Ren and P. Y. Papalambros, "Design of Hybrid-Electric Vehicle Architectures using Auto-Generation of Feasible Driving Modes," *ASME 2013 International Design Engineering Technical Conferences and Computers and Information in Engineering Conference, Portland,* pp. 1 - 9, August 2013.

[6] D. Cundev, Z. Cerovsky and P. Mindl, "Modeling of the Hybrid Electric Drive with an Electric Power Splitter and Simulation of the Fuel Efficiency," in *European Conference on Power Electronics and Applications*, Barcelona, pp. 1 - 10, September 2009.

[7] Z. Yang, F. Shang, I. Brown and M. Krishnamurthy, "Comparative Study of Interior Permanent Magnet, Induction, and Switched Reluctance Motor Drives for EV and

HEV Applications," *IEEE Transactions on Transportation Electrification,* vol. 1, no. 3, pp. 245-254, October 2015.

[8] A. Ansari, "Performance and Analysis with Power Quality Improvement with Induction Motor in Electric Drive," *International Journal of Engineering and Technical Research,* vol. 2, no. 10, pp. 30-34, October 2014.

[9] M. Kim, D. Jeung and K. Min, "Fuel Economy of Series Hybrid Electric Bus by Matching the Gear Ratio of Different Capacity Traction Motors," *World Electric Vehicle Journal,* vol. 5, no. 1, pp. 254-260, May 2012.

[10] I.-S. Kim, "Nonlinear State of Charge Estimator for Hybrid Electric Vehicle Battery," *IEEE Transactions on Power Electronics,* vol. 23, no. 4, pp. 2027-2034, July 2008.

[11] T. P. Hanusa, *The Lightest Metals: Science and Technology from Lithium to Calcium*, West Sussex, UK, John Wiley & Sons, 2015, pp. 310-311.

[12] H. M. E. Shewy, F. A. A. Kader, M. M. E. Kholy and A. E. shahat, "Dynamic Modeling of Permanent Magnet Synchronous Motor Using MATLAB - Simulink," *Proceedings of the 6th International Conference on Electrical Engineering (ICEENG),* pp. 1 - 16, May 2008.

[13] S. Delprat, "Control of a Parallel Hybrid Powertrain: Optimal Control," *IEEE Transactions on Vehicular Technology,* vol. 53, no. 3, pp. 872-881, May 2004.

[14] G.-S. Hwang, "Power Flows and Torque Analyses of an Independently Controllable Transmission with a Parallel Type," *Proceedings of the World Congress on Engineering, London, U.K.,* vol. 3, pp. 2020 - 2024, July 2011.

[15] R. Johri, "Simultaneous Optimization Of Supervisory Control And Gear Shift Logic For A Parallel Hydraulic Hybrid Refuse Truck Using Stochastic Dynamic

Programming," *ASME Dynamic Systems and Control Conference and Bath/ASME Symposium on Fluid Power and Motion Control,* pp. 99 - 106, 2011.

[16] M. H. Prins, C. W. Vorster and M. J. Kamper, "Reluctance Synchronous and Field Intensified-PM Motors for Variable-Gear Electric Vehicle Drives," *IEEE Energy Conversion Congress and Exposition,* pp. 657-664, September 2013.

[17] "United States Environmental Protection Agency - Dynamometer Drive Schedules," 2013. [Online]. Available: http://www3.epa.gov/nvfel/testing/dynamometer.htm#vehcycles.